# Numerical Investigation of Frequency Reconfigurable Antenna with Liquid Metamaterials for X-band

*Shobhit K. PATEL*[1,2], *Cong Danh BUI*[3,4], *Truong Khang NGUYEN*[3,4,*], *Juveriya PARMAR*[5], *Quang Minh NGO*[6,7]

[1]Department of Computer Engineering, Marwadi University, Rajkot, Gujarat, India.
[2]Electronics and Communication Department, Marwadi University, Rajkot, 360003, India
[3]Division of Computational Physics, Institute for Computational Science, Ton Duc Thang University, Ho Chi Minh City, Vietnam
[4]Faculty of Electrical and Electronics Engineering, Ton Duc Thang University, Ho Chi Minh City, Vietnam
[5]Physics Department, Marwadi University, Rajkot, 360003, India
[6]University of Science and Technology of Hanoi, Vietnam Academy of Science and Technology, 18 Hoang Quoc Viet, Cau Giay, Hanoi, Vietnam
[7]Institute of Materials Science, Vietnam Academy of Science and Technology, 18 Hoang Quoc Viet, Cau Giay, Hanoi, Vietnam

*Corresponding Author: Truong Khang NGUYEN (Email: nguyentruongkhang@tdtu.edu.vn)
(Received: 1-Jan-2022; accepted:14-Mar-2022; published: 31-March-2022)
http://dx.doi.org/10.55579/jaec.202261.362

***Abstract.*** *In this paper, a frequency reconfigurable liquid metamaterial microstrip-based radiating structure is proposed and it is an attempt towards achieving reconfiguration in liquid metamaterial-based microstrip radiating structures. Reconfigurable antenna design is superstrated with five liquid metamaterial layers based on a distilled water split-ring resonator. Superstrate layers give enhancement from 6.5 dB to 13.1 dB in the gain of the proposed antenna. A patch is reconfigured through PIN diodes as RF switches. Switching 'on' and 'off' states of PIN diodes are used for reconfiguration of frequency and radiation patterns. Analysis in terms of reflection coefficient, gain (dBi), radiation pattern, bandwidth (BW), and half-power beamwidth (HPBW) is obtained in switch-off and switch-on state. The proposed design provides enhanced gain, reflection coefficient, and multiband characteristics in the 8-12 GHz range suitable for X-band satellite and radar applications.*

***Keywords***

***Liquid metamaterial, reconfigurable antenna, radiating structure, multiband characteristics.***

## 1. Introduction

Antenna technology has advanced to its new heights with broadband and high gain antennas. High gain and broadband antennas can be designed using metamaterials. Metamaterials are artificial materials that possess unusual electromagnetic properties that can be applied to conventional antennas to improve their parameters such as bandwidth and gain. Bulk metamaterials are generally designed using two types of

 

structures, metamaterials using thin wires to obtain negative permittivity and using split-ring resonators (SRRs) to obtain negative permeability [1]. Split ring resonator-based metamaterials function as a magnetic dipole that can be excited by an axial magnetic field [2]. A broadband compact microstrip patch antenna design loaded with multiple split-ring resonator substrates and superstrates is presented. The analysis is obtained for two, three, and four ring SRR loaded in substrate and superstrate for small and large spacing between the rings. Results show that the loading of multiple SRR in the superstrate and substrate of the antenna increases the bandwidth of the antenna and a small gap SRR design gives better performance as compared to a large gap SRR design [3]. We have used the same concept of three-ring SRR in our proposed design because of its advantage in increasing bandwidth. A novel square-tooth split-ring resonator loaded in a substrate of the truncated square microstrip patch antenna is analyzed. This new type of metamaterials functions as a slow-wave structure and it provides improved radiation characteristics and bandwidth enhancement of about 20-30% as compared to simple split-ring resonators. Antennas loaded with corrugated split ring resonators provide enhanced gain and bandwidth performance as compared to conventional SRR based metamaterial loaded antenna structure [4, 5].

Metamaterials can be loaded in substrate, patch, and ground or as superstrate. Multiband characteristics are obtained in a meandered microstrip patch antenna by loading SRR inclusions studied in [6]. Truncated square microstrip antenna design with metallic SRR inclusion in substrate gives multiband characteristics. Two designs with different sized meandered slits with the same dimension of SRR are analyzed and have their results compared. Negative permittivity and permeability of the metamaterial for different bands are represented for both designs [7]. Radiation improvement in terms of gain is obtained as compared to the conventional patch antenna by metallic inclusion of SRR in the diamond substrate in the microstrip patch antenna design as studied in [8]. Enhancement of antenna performance in terms of bandwidth is obtained by adding metamaterial layers as a superstrate of the meandered microstrip patch antenna. As compared to conventional simple patch antenna without metamaterial superstrate layers, bandwidth enhancement of 11% to 60% along with improvement in reflection coefficient and Voltage Standing Wave Ratio (VSWR) is also presented [9]. It has been shown that the inclusion of SRR in the parallel plate structure improves its performance in terms of reflection coefficient and VSWR [10]. A comparative analysis of microstrip patch antenna superstrated with six metamaterial radome layers and that with four log-periodic metamaterial layers is obtained. The result shows that improved reflection coefficient, the gain is achieved in the four-layered metamaterial log-periodic radome design while the six-layered metamaterial radome design has maximum bandwidth [11]. A concept of periodic stacking of metasurface radome layers over microstrip antenna is introduced in [12] which provides enhanced gain, directivity, and efficiency as compared to simple multilayer metasurface radome layer design [13]-[17].

Liquid antennas are also getting attention from researchers as a low-cost alternative to the copper antenna. Liquid antennas are also designed to improve different antenna parameters. The metamaterials incorporated in conventional antennas can be designed with liquid materials to enhance different antenna parameters. A liquid monopole antenna is investigated in terms of resonant frequency, fractional bandwidth, and radiation efficiency. Results reveal that the dielectric layer between the water and the ground determines the resonant frequency and radiation efficiency by varying the conductivity of water. The antenna functions as a dielectric resonator antenna, conducting antenna, or as their combination [18]. The liquid antenna can improve the radiation of the normal patch antenna. The liquid metamaterials can be loaded in superstrate to improve the gain of the antenna. The use of liquid antennas gives flexibility in design with advantages of enhanced gain, bandwidth, etc. [19]-[22].

Reconfiguration in frequency and radiation pattern is very important in many wireless applications. This need has created new space for reconfigurable antennas. There are two ways to make a reconfigurable antenna, either using

discrete elements such as varactor, PIN diodes, and MEMS switches [23] or using tunable materials such as ferroelectric film, graphene, and liquid crystal [24]. A microstrip patch antenna design consisting of the dual patch, rectangular and U-shaped patch with three PIN diode switches between them is presented. Frequency reconfiguration is obtained by different switching conditions as the effective length of the antenna changes resulting from different current path lengths by switching [25]. Frequency reconfiguration is achieved by adding PIN diodes as switches in the space between the two patches. The comparative analysis is obtained for different switching conditions of the design with and without metamaterial and enhanced gain and reflection coefficient is obtained [26]. A microstrip patch antenna loaded with multiple split-ring resonators (MSRR) with RF-MEMS switches added in the gap of SRRs is studied. Frequency and radiation pattern is reconfigured by different switching states, no switch on, one switch ON, two switches ON, and three switches ON [27].

Reconfigurable antennas are important in many ways and several of these antennas are presented [28]-[32]. Reconfigurable cylindrical spiral and tapered helical water antenna are designed and fabricated. The radiation pattern is obtained by using 3.5% salinity of water and the direction of radiation pattern changes at the threshold ratio of spiral diameter and wavelength of 0.1 and 0.4 [28]. A dielectric resonator antenna (DRA) is composed of two parts, the inner part of the solid K9 glass and the outer part is filled with liquid ethyl acetate. When ethyl acetate is pumped out, the DRA is excited in broadside HEM11$\delta$ mode and when it is pumped in, the DRA is excited in conical TM01$\delta$ mode, and thus mode reconfiguration is obtained [29]. A frequency and pattern reconfigurable antenna based on liquid crystal (LC) technology is designed which consists of a microstrip patch array and an inverted microstrip line (IMSL). The resonance frequency is changed by LC substrate and LC-based IMSL phase shifter tunes the transmission phase by changing the effective permittivity of LC [24]. Beam scanning reflectarrays based on LCs are designed with the unit cell structure consisting of three coplanar dipoles. Resonant frequency and phase are reconfigured by varying the permittivity of the LC and thus this antenna is a potential candidate for satellite applications [30]. A novel tunable antenna using K15 LC design provides enhanced frequency tuning range, impedance bandwidth, efficiency, and gain as compared to conventional antenna design [31]. The concept of nematic liquid crystal-based metasurface structure arranged periodically to electronically reconfigure antenna performance is presented. Due to the dielectric anisotropy property of liquid crystals, as DC control voltage is changed corresponding reflection phase of the structure changes and thus it is reconfigurable [32].

The concept of liquid metamaterials in antenna technology provides extraordinary results which are merely not achieved by metal metamaterials. Microstrip patch antenna loaded with a novel corrugated SRR design superstrated with liquid metamaterial radome structure provides improved bandwidth, reflection coefficient, and gain as studied in [33]. Multiband reconfigurable patch antenna based on multiple complementary split-ring resonators provided enhanced gain and tunability [34]. Microstrip patch antenna with Rogers substrate is loaded with distilled water SRR, seawater SRR, and copper SRR. Comparative analysis of these three designs is obtained which shows that maximum bandwidth and gain is obtained in seawater SRR based design, the optimum reflection coefficient is obtained in copper SRR based design and the maximum number of bands in distilled water SRR based design [13]. Broadband and high gain characteristics are obtained in liquid metamaterial-based radome design. In [34], square and circular thin wire-based metamaterial using freshwater, distilled water, and seawater are reported and their comparative analysis in terms of reflection coefficient, bandwidth, and gain is obtained.

The need for frequency reconfiguration and high gain is increasing day by day in antenna design technology, especially in modern and advanced wireless communication [35, 36]. These requirements can be fulfilled by incorporating new materials and different switching techniques in the microstrip patch antenna. In this paper, we present a liquid metamaterial microstrip antenna to achieve frequency reconfiguration

which helps in enhancing the design performance. The paper is organized as follows. The design and structure of the reconfigurable liquid metamaterial-based antennas are presented in section 2. Results and discussion is presented in section 3 and finally, the conclusion is presented in section 4.

## 2. Design and modelling

In this section, we present a liquid reconfigurable metamaterial radome design consisting of a reconfigurable microstrip patch antenna superstrated with five liquid metamaterial radome layers. The schematic representation of the design is shown in Fig. 1. The antenna design consists of reconfigurable patch, Rogers RT/Duroid 5880 substrate having a relative permittivity of 2.2 and ground layer. The patch is reconfigured through PIN diodes as RF switches connected to inner and outer patches. Inner and outer patch dimensions are 56.4×56.4×0.5 $mm^3$ and 70×70×0.5$mm^3$ respectively and substrate size is 216.4×216.4×1.5 $mm^3$. Fig. 1-(a) and Fig. 1-(b) show the top view of the design in switch OFF state and switch ON state respectively and Fig. 1-(c) shows the side view of the design. Five metamaterial radome layers as superstrate over the antenna are designed with a split ring resonator (SRR) of distilled water over the Rogers RT/Duroid 5880 substrates. The sizes of the three rings in the SRR are 28×28×0.5 $mm^3$, 20×20×0.5 $mm^3$, and 12×12×0.5 $mm^3$ respectively and the width of the SRR ring is 4 mm. The thickness of the radome layer is 2 mm, the spacing between the radome layers and the antenna is 9.5 mm, and that between consecutive radome layers is 3.5 mm. The port is applied at one side of the patch with 25 mm and 25 mm according to $x$ and $y$ positions, respectively. The antenna operates in two conditions: i) State A: when the switch is OFF, ii) State B: when the switch is ON. In-state A, the inner patch acts as a radiator and it is not connected to the outer patch. In-state B both outer patch and inner patch radiate as they are connected through switches. SRR is designed with distilled water as it shows improved performance over fresh water and seawater to obtain multiband characteristics [13].

The equivalent circuit representation of the SRR consists of equivalent inductance (L) per unit length and capacitances ($C_{12}$ and $C_{23}$) as shown in Fig. 2. The ring of the SRR has equivalent inductance L and into equivalent capacitances, $C_{12}$ and $C_{23}$ between the three rings in SRR respectively. If the length of the ring is $b$, the width of the ring is $a$, the gap between the split of ring is $g$, the thickness of the ring is $t$, the permittivity of the SRR material is $\varepsilon$ and $\mu_0$ is free space permeability then inductance $L$ per unit length and series capacitance $C_S$ can be obtained from equations (1) and (2) respectively [3].

$$L = \frac{\mu_0 b}{\sqrt{\pi}} \left[ \log\left( \frac{32b}{a\sqrt{\pi}} \right) - 2 \right] \tag{1}$$

$$C_s = \varepsilon \frac{at}{2g} \tag{2}$$

The series capacitance $C_S$ of the SRR resulting from the upper and lower halves of the SRR is related to the mutual capacitance between the three rings $C_{12}$ and $C_{23}$ as Eq. (3). The resonant frequency of the SRR can be obtained from Eq. (4) [3]. In this paper, dimensions of the SRR are taken as $a$ = 4 mm, $g$ = 2 mm, $t$ = 0.5 mm and $b$ for the three rings are 28, 20, and 12 mm respectively.

$$C_S = \frac{(C_{12} + C_{23})}{4} \tag{3}$$

$$f = \frac{1}{2\pi\sqrt{LC_S}} \tag{4}$$

In this design, patch size is reconfigured through pin Diodes as RF switches and hence frequency reconfiguration is obtained. The PIN diode is used as it functions as an efficient RF switch due to the large amount of charge storage in the intrinsic region between the two junctions. The proposed design is simulated in High-Frequency Structure Simulator (HFSS). Figure 3-(a) represents the HFSS PIN Diode model as RF switch between two metal contacts in terms of lumped RLC boundaries. Equivalent circuit representation in switch ON state is a series combination of resistor ($R_S$) and inductor (L) while in switch OFF state is a parallel combination of capacitor ($C_P$) and resistor ($R_P$) which is in series with

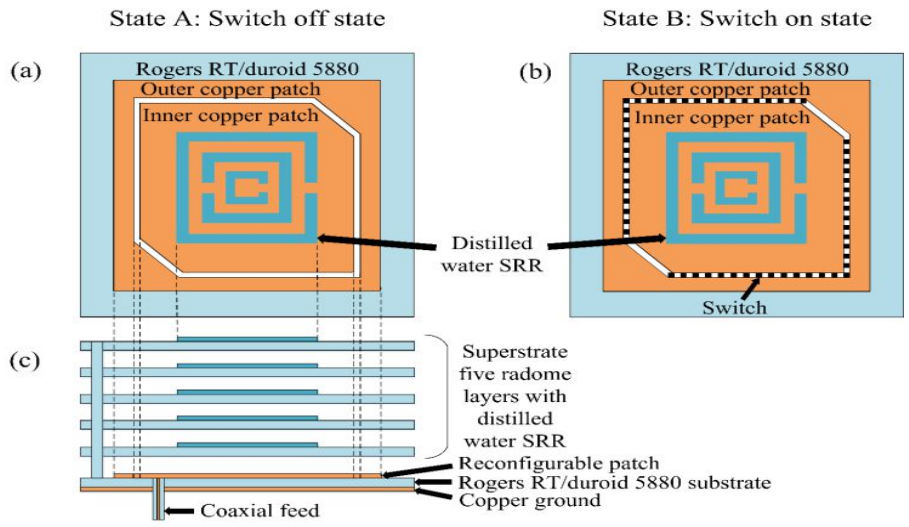


**Fig. 1:** Representation of reconfigurable microstrip patch antenna superstrated with five liquid metamaterial radome layers as superstrate, (a) top view in switch OFF state (State A), (b) top view in switch ON state (State B), (c) side view.

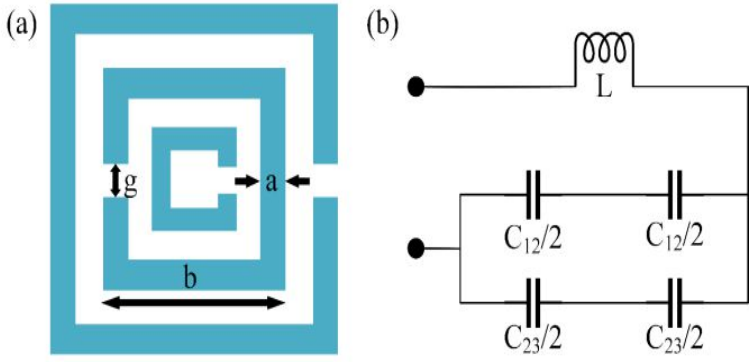


**Fig. 2:** Equivalent circuit representation of split-ring resonator. (a) SRR and (b) equivalent circuit representation of SRR.

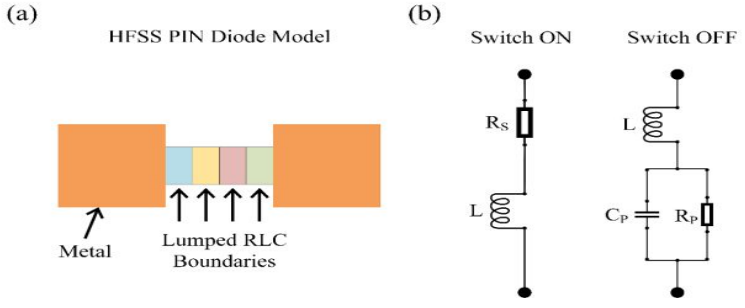


**Fig. 3:** (a) PIN Diode HFSS model as RF switch represented through lumped RLC boundaries between two metal contacts (b) Equivalent circuit representation of PIN Diode switch in ON and OFF state in terms of RLC components.

inductor (L) as represented in Fig. 3-(b). In switch ON state, RL circuit allows the current to flow between the two metallic contacts and in switch OFF state capacitor blocks the current [25, 26]. The PIN diode is forward-biased with 0.7 V and 10 mA. The PIN diode exhibits an ohmic resistance of 3.0 Ω and intrinsic capacitance of 0.1 pF for the forward bias, but 2.7 kΩ and 9.0 pF at 0 V.

## 3. Result and discussion

In this section, simulation results of the proposed frequency reconfigurable liquid metamaterial microstrip based radiating structure is presented in terms of reflection coefficient, 3-dB rectangular gain, radiation pattern, and polar gain plot in switch ON and OFF conditions. Figure 4represents a comparative analysis of reflection coefficient ($S_{11}$(dB)) obtained for the proposed design in switch ON and switch OFF state in 8 GHz to 12 GHz frequency range. This result represents resonant frequency reconfiguration as a frequency shift is observed. Considering frequency bandwidth for $|S_{11}(dB)| <$ -10dB, four frequency bands are obtained in switch OFF state at the central frequency of 8.725 GHz, 9.189 GHz, 10.362 GHz and 10.920 GHz and corresponding reflection coefficient obtained are -33.236 dB, -13.412 dB, -18.614 dB and -12.322 dB respectively. In switch ON state, three frequency bands are obtained at the central frequency of 8.812 GHz, 9.999 GHz, and 11.147 GHz and corresponding reflection coefficients obtained are -13.385 dB, -18.448 dB, and -23.046 dB respectively. Multiband characteristic of the antenna is observed in this reconfigurable radiating structure. The shift in the frequency is visible in Fig. 4. All four bands are shifted by two states of diode switches. The maximum frequency shift of 350 MHz is visible in the third band around 10 GHz frequency band. The stacking of metamaterial radome layers has the advantage of increased gain characteristics and so in this design, five radome layers are used. The gain is enhanced with superstrate layers. The gain without superstrate layer is 6.5 dB and gain with superstrate layer is enhanced to 13.1 dB which is presented in detail below.

Analysis of 3-dB gain to obtain HPBW for all multiband responses is observed in the switch ON and switch OFF state. Far-field gain plot (dBi) in switch OFF state is represented in Fig. 5. Far-field 3-dB gain at the central frequency of 8.725 GHz, is obtained at $\theta$ = -67$^o$ to -40$^o$ range, at 9.189 GHz is obtained at $\theta$ = -15$^o$ to 12$^o$, at 10.362 GHz is obtained at $\theta$ = -52$^o$ to -31$^o$ and at 10.920 GHz is obtained at $\theta$ = -18$^o$ to -5$^o$ range. Thus, corresponding HPBW is obtained as 27$^o$, 27$^o$, 21$^o$, and 13$^o$ respectively. Similarly, for switch ON state, far-field gain plot (dB) is reported in Fig. 6. It is observed that at the central frequency of 8.812 GHz, the 3-dB gain is obtained at $\theta$ = -12$^o$ to 9$^o$ with HPBW of 21$^o$. Also, at 9.999 GHz and 11.147 GHz band, the 3-dB gain is achieved at $\theta$ = -78$^o$ to -59$^o$ and $\theta$ = 44$^o$ to 60$^o$ with the corresponding HPBW of 19$^o$ and 16$^o$ respectively. Generally, the HPBW presented in Figs. 5 and 6 clearly shows the directiveness of the antenna where the beamwidths are sharp and multiple beams are visible because of the use of multiple layers of the radome design. Theoretically, the lower the value of HPBW show more directive the antenna and thus producing higher directivities. This behavior is significant in finding out the gain and range of the antenna. On the other hand, the higher directive antennas are applicable for long-distance communications. Moreover, it can be seen in Fig. 6 for the switching ON state that narrower HPBW was obtained at the broadside direction, i.e., 0 degree, in a comparison to the one in Fig. 5 for the switching OFF state. This observation indicates that the beam collimation in ON state was better than that in OFF state.

Gain polar plot (dBi) in switch OFF state is reported in Fig. 7. Total gain obtained at frequency f = 8.725 GHz, 9.189 GHz, 10.362 GHz and 10.920 GHz are 11.813 dB, 10.860 dB, 9.9385 dB and 13.130 dB represented in Fig. 7-(a), 7-(b), 7-(c) and 7-(d), respectively. Figure 8 represents the gain polar plot (dB) in switch ON state. Total gain obtained at frequency f = 8.812 GHz, 9.999 GHz and 11.147 GHz are 10.216 dB, 10.422 dB and 11.164 dB as shown in Fig. 8-(a), 8-(b) and 8-(c), respectively. This result represents reconfiguration in terms of gain

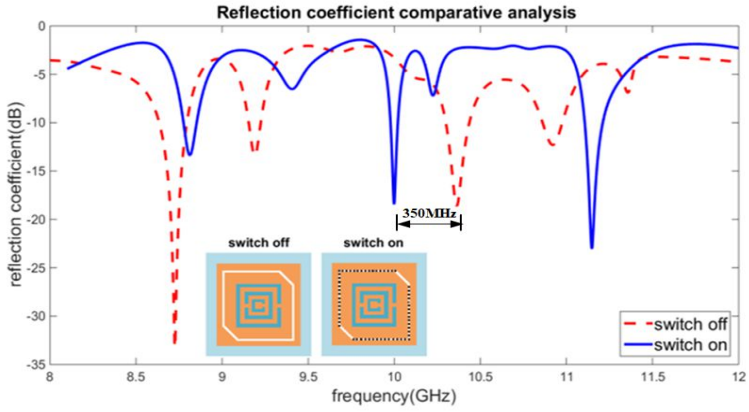


**Fig. 4:** Reflection coefficient (dB) comparative analysis in switch OFF and switch ON state showing reconfiguration in terms of the resonant frequency. The inset figure shows two states of operation for which results are obtained. The maximum reconfiguration of 350 MHz is visible between the switch off and switch on states of diodes.

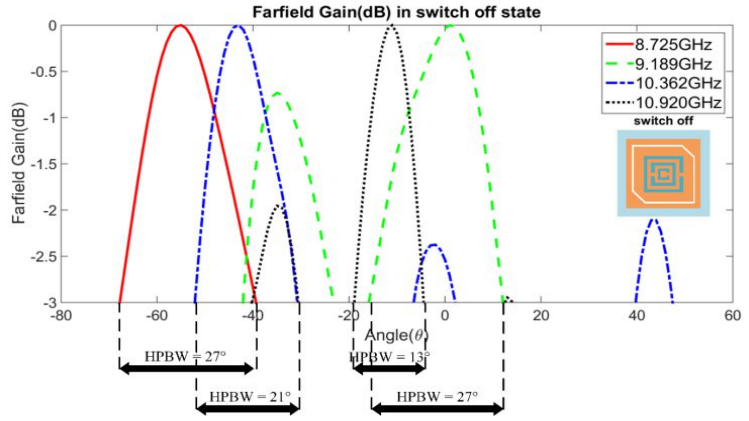


**Fig. 5:** Far-field gain plot (dBi) in switch OFF state for multiband responses observed at 8.725 GHz, 9.189 GHz, 10.362 GHz, and 10.920 GHz. The half-power beamwidth (HPBW) ranges from $13^o$ to $27^o$.

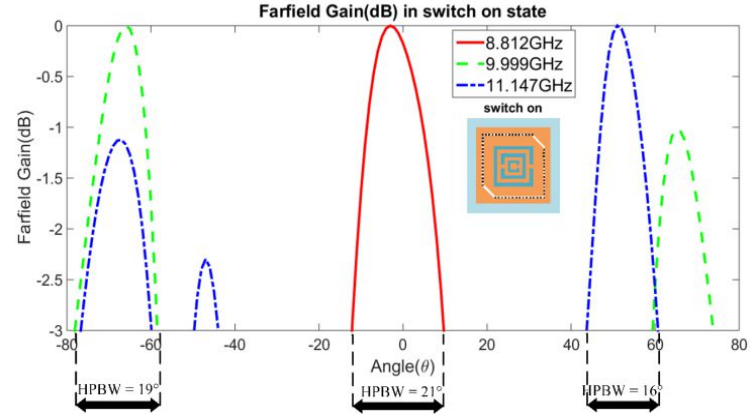


**Fig. 6:** Far-field gain plot (dBi) in switch ON state for multiband responses observed at 8.812 GHz, 9.999 GHz and 11.147 GHz.

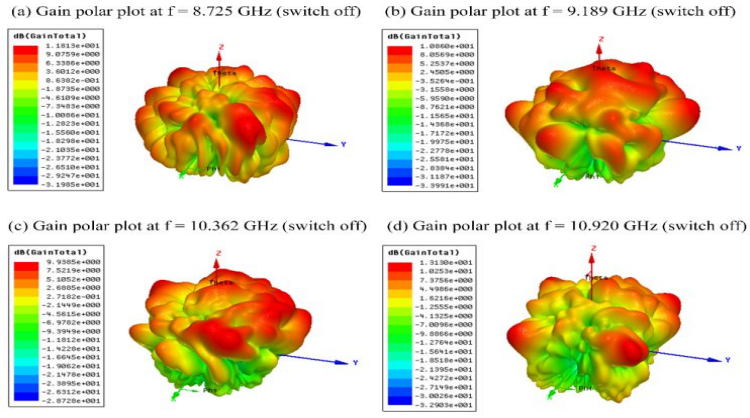


**Fig. 7:** Gain polar plot (dBi) in switch OFF state. Gain (dBi) at frequency, (a) f = 8.725 GHz is 11.813 dB, (b) 9.189 GHz is 10.860 dB, (c) 10.362 GHz is 9.9385 dB and (d) 10.920 GHz is 13.130 dB.

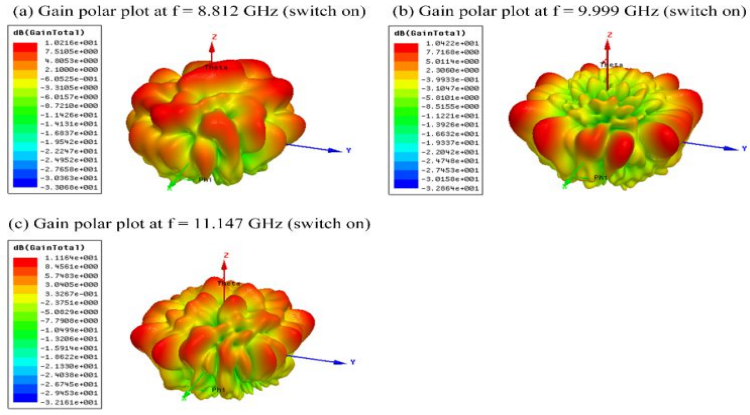


**Fig. 8:** Gain polar plot (dB) in switch ON state. Gain (dB) at frequency, (a) f = 8.812 GHz is 10.216 dB, (b) 9.999 GHz is 10.422 dB and (c) 11.147 GHz is 11.164 dB.

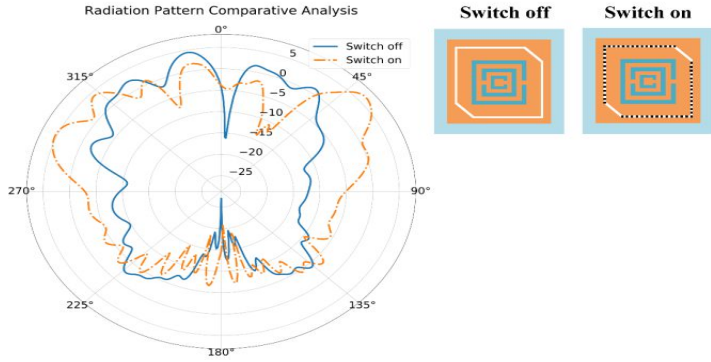


**Fig. 9:** Radiation pattern (dB) in switch OFF state at 10.920 GHz and in switch ON state at 11.147 GHz. Inset figure shows two states of operation for which results are obtained.

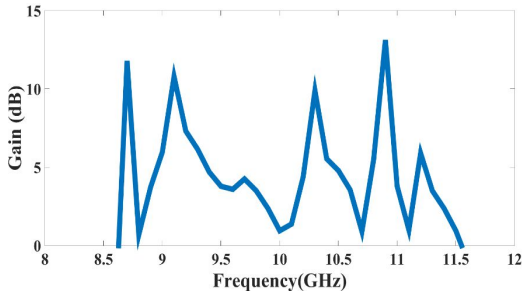


**Fig. 10:** Radiation pattern (dB) in switch OFF state at 10.920 GHz and in switch ON state at 11.147 GHz. Inset figure shows two states of operation for which results are obtained.

**Tab. 1:** Reconfiguration in antenna parameters and comparative analysis representation in terms of resonant frequency, reflection coefficient, bandwidth, gain total and HPBW.

| Frequency Band (switch off/on) | Size ($mm^2$) | Resonant frequency (GHz) | S11 (dB) | BW (MHz) | Gain total (dBi) | HPBW |
|---|---|---|---|---|---|---|
| Band 1 (switch off) | 56.4×56.4 | 8.725 | -33.23 | 157 | 11.813 | $27^o$ |
| Band 1 (switch on) | 56.4×56.4 | 8.812 | -13.385 | 73 | 10.216 | $21^o$ |
| Band 2 (switch off) | 56.4×56.4 | 9.189 | -13.412 | 67 | 10.860 | $27^o$ |
| Band 2 (switch on) | 56.4×56.4 | 9.999 | -18.448 | 42 | 10.422 | $19^o$ |
| Band 3 (switch off) | 56.4×56.4 | 10.362 | -18.614 | 132 | 9.9385 | $21^o$ |
| Band 3 (switch on) | 56.4×56.4 | 11.147 | -23.046 | 104 | 11.164 | $16^o$ |
| Band 4 (switch off) | 56.4×56.4 | 10.920 | -12.322 | 114 | 13.130 | $13^o$ |

in the switch OFF and switch ON state of the proposed design. It is observed here, that maximum gain in switch OFF state is obtained at 10.920 GHz and that in switch ON state is observed at 11.147 GHz. The radiation pattern at these two frequencies in switch OFF and ON state is represented in Fig. 9 which shows reconfiguration in the radiation pattern. The far-field shape shows multibeam behavior because of multiple layers of the radome design.

Hence, maximum coplanar gain (dBi) in switch OFF state is obtained at 8.725 GHz and that in switch ON state is obtained at 8.812 GHz. A comparative analysis of radiation pattern at these two frequencies in switch OFF and switch ON state respectively is represented in Fig. 9 which represents a reconfiguration of the radiation pattern. The directivity of the radiation beam is increased for the switch-off state of the diode compared to the switch-on state. The gain plots for different frequency ranges are also provided in Fig. 10 to show the improvement in gain at different frequencies. The gain is highest at 10.920 GHz with 13.1 dB values.

Comparative analysis of all results of the proposed reconfigurable liquid metamaterial-based radiating structure design in terms of resonant frequency, reflection coefficient, bandwidth (BW), gain total (dB), and HPBW in switch OFF and ON state is represented in Tab. 1. All these parameters are analyzed for multiple bands obtained in the switch ON and OFF state. It is observed that resonant frequencies are shifted in the switch OFF and switch ON state from 8.725 GHz to 8.812 GHz, 9.189 GHz to 9.999 GHz, and 10.362 GHz to 11.147 GHz respectively. The optimum reflection coefficient of -33.236 dB and bandwidth of 157 MHz is achieved at 8.725 GHz in band1 in switch OFF state. The maximum total gain of 13.130 dB is obtained at 10.920 GHz in band4 in switch OFF state. A minimum of $13^o$ is achieved at 10.920 GHz in switch OFF state. It is noticeable that for all bands, HPBW is decreased in switch ON state as compared to switch ON state.

The proposed design gain is compared with previously published similar designs [34]-[38] in Tab. 2. The comparison clearly shows the en-

 

hancement in the gain in our design compared to other designs.

**Tab. 2:** The comparison of proposed design gain with previously published similar designs [34]-[38].

| Design | Size ($mm^2$) | Gain (dB) |
|---|---|---|
| Frequency selective microstrip antenna design from [37] | 25×23 | 7.2 |
| Microstrip antenna design from [38] | 51.1×39.8 | 7.8 |
| High gain antenna with metasurface design from [39] | 78×78 | 8.2 |
| Liquid radome design from [40] | 9.5×9.5 | 8.3 |
| Reconfigurable high gain antenna design from [41] | 39.6×39.6 | 10.6 |
| Proposed design | 56.4 ×56.4 | 13.1 |

# 4. Conclusion

We conclude that the proposed frequency reconfigurable liquid metamaterial microstrip-based radiating structure is designed and results are obtained in terms of reflection coefficient, bandwidth, gain, HPBW, and radiation patterns. Enhanced antenna parameter along with reconfiguration characteristics of the antenna is achieved. Multiband and high gain are achieved due to liquid metamaterials and implementation of switches enables to reconfigure the proposed radiating structure. The superstrate layer improves the gain from 6.5 dB to 13.1 dB. Four frequency bands are achieved in the switch OFF state and three bands in the switch ON state. The maximum reflection coefficient and bandwidth of -33.236 dB and 157 MHz is achieved at 8.725 GHz in switch OFF state. The maximum gain of 13.130 dB is obtained at 10.920 GHz in switch OFF state. The maximum tuning of 350 MHz is achieved using PIN diode switches. HPBW seems to decrease or directivity of the proposed design increases in switch ON state as compared to switch OFF state. The proposed design is suitable for certain X-band applications in 8-12 GHz of the frequency range.

# Acknowledgement

This research is funded by Vietnam National Foundation for Science and Technology Development (NAFOSTED) under grant number 102.04-2019.04.

# References

[1] Engheta, N., & Ziolkowski, R. W. (Eds.). (2006). Metamaterials: physics and engineering explorations. John Wiley & Sons.

[2] Velez, A., Aznar, F., Bonache, J., Velázquez-Ahumada, M. C., Martel, J., & Martín, F. (2009). Open complementary split ring resonators (OCSRRs) and their application to wideband CPW band pass filters. IEEE Microwave and Wireless Components Letters, 19(4), 197-199.

[3] Patel, S. K., Argyropoulos, C., & Kosta, Y. P. (2017). Broadband compact microstrip patch antenna design loaded by multiple split ring resonator superstrate and substrate. Waves in Random and Complex Media, 27(1), 92-102.

[4] Kriegler, C. E., Rill, M. S., Thiel, M., Müller, E., Essig, S., Frölich, A., ... & Wegener, M. (2009). Transition between corrugated metal films and split-ring-resonator arrays. Applied Physics B, 96(4), 749-755.

[5] Ding, Y., Li, M., Chang, H. X., & Qin, K. (2014). A dual-band high gain antenna based on split ring resonators and corrugated plate. Progress In Electromagnetics Research Letters, 44, 87-92.

[6] Xu, X., Huang, Q., Deng, X., & Wang, Y. (2019). Electric megahertz metamaterials designed with deep subwavelength multilayered meander line resonators. Journal of Applied Physics, 125(19), 194902.

[7] Cao, W. Q., Liu, A. J., Zhang, B. N., Yu, T. B., Guo, D. S., Wei, Y., & Qian, Z. P. (2012). Multi-band multi-mode microstrip circular patch antenna loaded with metamaterial structures. Journal of Electromagnetic Waves and Applications, 26(7), 923-931.

[8] Singh, A. K., Abegaonkar, M. P., & Koul, S. K. (2018). Miniaturized multiband microstrip patch antenna using metamaterial loading for wireless application. Progress In Electromagnetics Research C, 83, 71-82.

[9] Kushwaha, R. K., Karuppanan, P., & Srivastava, Y. (2018). Proximity feed multiband patch antenna array with SRR and PBG for THz applications. Optik, 175, 78-86.

[10] Roy, S., & Chakraborty, U. (2020). Metamaterial-embedded dual wideband microstrip antenna for 2.4 GHz WLAN and 8.2 GHz ITU band applications. Waves in Random and Complex Media, 30(2), 193-207.

[11] Patel, S. K., Shah, K. H., & Kosta, Y. P. (2018). Multilayer liquid metamaterial radome design for performance enhancement of microstrip patch antenna. Microwave and Optical Technology Letters, 60(3), 600-605.

[12] He, Y., & Eleftheriades, G. V. (2019). A thin double-mesh metamaterial radome for wide-angle and broadband applications at millimeter-wave frequencies. IEEE Transactions on Antennas and Propagation, 68(3), 2176-2185.

[13] Patel, S. K., & Kosta, Y. (2018). Liquid metamaterial based microstrip antenna. Microwave and Optical Technology Letters, 60(2), 318-322.

[14] Zharov, A. A., & Zharova, N. A. (2014). Liquid metacrystals. JOSA B, 31(3), 559-564.

[15] Patel, S. K., & Argyropoulos, C. (2016). Enhanced bandwidth and gain of compact microstrip antennas loaded with multiple corrugated split ring resonators. Journal of ElEctromagnEtic WavEs and applications, 30(7), 945-961.

[16] Deng, G., Lu, Y., Yin, Z., Lai, W., Lu, H., Yang, J., ... & Chi, B. (2018). A tunable polarization-dependent terahertz metamaterial absorber based on liquid crystal. Electronics, 7(3), 27.

[17] Patel, S. K., & Kosta, Y. (2013). Investigation on radiation improvement of corner truncated triband square microstrip patch antenna with double negative material. Journal of Electromagnetic Waves and Applications, 27(7), 819-833.

[18] Xing, L., Huang, Y., Shen, Y., Al Ja'afreh, S., Xu, Q., & Alrawashdeh, R. (2015). Further investigation on water antennas. IET Microwaves, Antennas & Propagation, 9(8), 735-741.

[19] Lavadiya, S. P., Patel, S. K., & Maria, R. (2021). High gain and frequency reconfigurable copper and liquid metamaterial tooth based microstrip patch antenna. AEU-International Journal of Electronics and Communications, 137, 153799.

[20] Huang, Y., Xing, L., Song, C., Wang, S., & Elhouni, F. (2021). Liquid antennas: Past, present and future. IEEE Open Journal of Antennas and Propagation.

[21] Keerthi, R. S., Dhabliya, D., Elangovan, P., Borodin, K., Parmar, J., & Patel, S. K. (2021). Tunable high-gain and multiband microstrip antenna based on liquid/-copper split-ring resonator superstrates for C/X band communication. Physica B: Condensed Matter, 618, 413203.

[22] Li, L., Yan, X., Zhang, H. C., & Wang, Q. (2021). Polarization-and Frequency-Reconfigurable Patch Antenna Using Gravity-Controlled Liquid Metal. IEEE Transactions on Circuits and Systems II: Express Briefs.

[23] Tran, H. H., Nguyen-Trong, N., Nguyen, T. K., & Abbosh, A. M. (2018). Bandwidth enhancement utilizing bias circuit as parasitic elements in a reconfigurable circularly polarized antenna. IEEE Antennas and Wireless Propagation Letters, 17(8), 1533-1537.

 

[24] Zhao, Y., Huang, C., Qing, A. Y., & Luo, X. (2017). A frequency and pattern reconfigurable antenna array based on liquid crystal technology. IEEE photonics journal, 9(3), 1-7.

[25] Nazir, I., Rana, I. E., Mir, N. U. A., & Afreen, K. (2016). Design and analysis of a frequency reconfigurable microstrip patch antenna switching between four frequency bands. Progress In Electromagnetics Research C, 68, 179-191.

[26] Patel, S. K., Shah, K. H., & Kosta, Y. P. (2019). Frequency-reconfigurable and high-gain metamaterial microstrip-radiating structure. Waves in Random and Complex Media, 29(3), 523-539.

[27] Patel, S. K., Argyropoulos, C., & Kosta, Y. P. (2018). Pattern controlled and frequency tunable microstrip antenna loaded with multiple split ring resonators. IET Microwaves, Antennas & Propagation, 12(3), 390-394.

[28] Li, G., Gao, G., Liu, W., & Tian, Z. (2017). Tunable and flexible liquid spiral antennas. Electronics Letters, 53(10), 648-650.

[29] Chen, Z., & Wong, H. (2017). Wideband glass and liquid cylindrical dielectric resonator antenna for pattern reconfigurable design. IEEE Transactions on Antennas and Propagation, 65(5), 2157-2164.

[30] Cuppo, F. L. S. A., Neto, A. M. F., Gómez, S. L., & Palffy-Muhoray, P. (2002). Thermal-lens model compared with the Sheik-Bahae formalism in interpreting Z-scan experiments on lyotropic liquid crystals. JOSA B, 19(6), 1342-1348.

[31] Dai, J. W., Peng, H. L., Zhang, Y. P., & Mao, J. F. (2017). A novel tunable microstrip patch antenna using liquid crystal. Progress In Electromagnetics Research C, 71, 101-109.

[32] Ma, S., Yang, G. H., Erni, D., Meng, F. Y., Zhu, L., Wu, Q., & Fu, J. H. (2017). Liquid crystal leaky-wave antennas with dispersion sensitivity enhancement. IEEE Transactions on Components, Packaging and Manufacturing Technology, 7(5), 792-801.

[33] Patel, S. K., Kosta, Y. P., & Charola, S. (2018). Liquid metamaterial based radome design. Microwave and Optical Technology Letters, 60(9), 2303-2309.

[34] Nguyen, T. K., Patel, S. K., Lavadiya, S., Parmar, J., & Bui, C. D. (2022). Design and fabrication of multiband reconfigurable copper and liquid multiple complementary split-ring resonator based patch antenna. Waves in Random and Complex Media, 1-24.

[35] Karthika, K., & Kavitha, K. (2021). Reconfigurable antennas for advanced wireless communications: A review. Wireless Personal Communications, 120(4), 2711-2771.

[36] AL-Fadhali, N., Majid, H. A., Omar, R., Abdul Sukor, J., Rahim, M. K., Zainal Abidin, Z., ... & Abo Mosali, N. (2021). Review on frequency reconfigurable antenna using substrate-integrated waveguide for cognitive radio application. Journal of Electromagnetic Waves and Applications, 35(7), 958-990.

[37] Bakr, M. S., Großwindhager, B., Rath, M., Kulmer, J., Hunter, I. C., Abd-Alhameed, R. A., ... & Bösch, W. (2019). Compact broadband frequency selective microstrip antenna and its application to indoor positioning systems for wireless networks. IET microwaves, antennas & propagation, 13(8), 1142-1150.

[38] Hassan, N., Zakaria, Z., Sam, W. Y., Hanapiah, I. N. M., Mohamad, A. N., Roslan, A. F., ... & Abd Aziz, M. Z. A. (2019). Design of dual-band microstrip patch antenna with right-angle triangular aperture slot for energy transfer application. International Journal of RF and Microwave Computer-Aided Engineering, 29(1), e21666.

[39] Pan, Y. M., Hu, P. F., Zhang, X. Y., & Zheng, S. Y. (2016). A low-profile high-gain and wideband filtering antenna with metasurface. IEEE Transactions on Antennas and Propagation, 64(5), 2010-2016.

[40] Patel, S. K., Shah, K. H., & Sonagara, J. S. (2020). Broadband liquid metamaterial radome design. Waves in Random and Complex Media, 30(2), 328-339.

[41] Chen, Q., Li, J. Y., Yang, G., Cao, B., & Zhang, Z. (2019). A polarization-reconfigurable high-gain microstrip antenna. IEEE Transactions on Antennas and Propagation, 67(5), 3461-3466.

## About Authors

**Shobhit K. PATEL** has done his Ph.D. on Electronics & communication engineering at Charotar University of Science and Technology, Changa, India. He is currently working in the area of photonics, metamaterial, antenna, optics and artificial intelligence. He has published several research papers in high impact SCI journals. He has also filed 7 Indian patents on different novel research done by him. He received DST international travel grant in the year 2014 to present a paper in IEEE APSURSI symposium at Memphis, USA. He also received DST International Travel Grant in the year 2017 to present a paper in PIERS Symposium, NTU, Singapore. He has been named in the list of "top 2% scientist worldwide identified by Stanford university" in 2021. He is currently working on many graphene-based projects and has received funding from SERB, DST, for his research. He has been honored with awards for the achievements in the area of the research field.

**Cong Danh BUI** received the B.S. degree in electronics and telecommunications from the Ho Chi Minh University of Science and Technology, Vietnam, in 2018. He is currently pursuing the master's degree with the Faculty of Electrical and Electronics Engineering, Ton Duc Thang University, Ho Chi Minh City, Vietnam. His current research interests include circularly polarized antennas, metamaterial-based antennas, and reconfigurable antennas.

**Truong Khang NGUYEN** received the B.S. degree in computational physics from the University of Science, Vietnam National University, Ho Chi Minh City, Vietnam, in 2006, and the M.S. and Ph.D. degrees in electrical and computer engineering from Ajou University, Suwon, South Korea, in 2013. From October 2013 to December 2014, he worked at the Division of Energy Systems Research, Ajou University, as a Postdoctoral Fellow. He is currently an Assistant Director and the Head of Division of Computational Physics at the Institute for Computational Science, Ton Duc Thang University, Ho Chi Minh City, and also a Managing Editor of the Journal of Advanced Engineering and Computation. He has authored or coauthored 70 peer-reviewed ISI journal articles and 40 conference papers. He has written one book chapter in the area of terahertz antenna and led one patent on terahertz stripline antenna. His current research interests include microwave antenna for wireless communication, terahertz antenna for compact and efficient source, nano structures and nano antenna for optical applications, and computational micro/nano fluidics.

**Quang Minh NGO** received his PhD in electrical engineering at Ajou University, the Republic of Korea in 2011. From March 2012 to January 2019, he worked as the Director of the Department of Materials and Engineering of Optical Fibers, Institute of Materials Science, Vietnam Academy of Science and Technology (VAST), Hanoi, Vietnam. Since February 2019, he has joined the University of Science and Technology of Hanoi, VAST as Vice Director of the Department of Aeronautics. He is an author/coauthor of more than 70 ISI papers. His main research focuses on design, simulation, fabrication and characterization of micro- and nanophotonics in the visible and near-infrared spectral regions for optical devices.